Environmental Engineering Research

Environ. Eng. Res. 2014 June,19(2) : 157-163

Research Paper

http://dx.doi.org/10.4491/eer.2014.19.2.157
pISSN 1226-1025 eISSN 2005-968X

# Batch and Flow-Through Column Studies for Cr(VI) Sorption to Activated Carbon Fiber

**In Lee, Jeong-Ann Park, Jin-Kyu Kang, Jae-Hyun Kim, Jeong-Woo Son, In-Geol Yi, Song-Bae Kim†**

*Environmental Functional Materials & Biocolloids Laboratory, Seoul National University, Seoul 151-921, Korea*

## Abstract

The adsorption of Cr(VI) from aqueous solutions to activated carbon fiber (ACF) was investigated using both batch and flow-through column experiments. The batch experiments (adsorbent dose, 10 g/L; initial Cr(VI) concentration, 5–500 mg/L) showed that the maximum adsorption capacity of Cr(VI) to ACF was determined to 20.54 mg/g. The adsorption of Cr(VI) to ACF was sensitive to solution pH, decreasing from 9.09 to 0.66 mg/g with increasing pH from 2.6 to 9.9; the adsorption capacity was the highest at the highly acidic solution pHs. Kinetic model analysis showed that the Elovich model was the most suitable for describing the kinetic data among three (pseudo-first-order, pseudo-second-order, and Elovich) models. From the nonlinear regression analysis, the Elovich model parameter values were determined to be $\alpha$ = 162.65 mg/g/h and $\beta$ = 2.10 g/mg. Equilibrium isotherm model analysis demonstrated that among three (Langmuir, Freundlich, Redlich–Peterson) models, both Freundlich and Redlich–Peterson models were suitable for describing the equilibrium data. In the model analysis, the Redlich–Peterson model fit was superimposed on the Freundlich fit. The Freundlich model parameter values were determined to be $K_F$ = 0.52 L/g and $1/n$ = 0.56. The flow-through column experiments showed that the adsorption capacities of ACF in the given experimental conditions (column length, 10 cm; inner diameter, 1.5 cm; flow rate, 0.5 and 1.0 mL/min; influent Cr(VI) concentration, 10 mg/L) were in the range of 2.35–4.20 mg/g. This study demonstrated that activated carbon fiber was effective for the removal of Cr(VI) from aqueous solutions.

**Keywords:** Activated carbon fiber, Adsorption, Batch experiment, Chromium, Flow-through experiment

## 1. Introduction

Chromium (Cr) is a metallic element widely present in the earth. It is essential for metabolism of plants and animals, but, at certain high level, may cause health problems, such as skin dermatitis, bronchitis, diarrhea, haemorrhage, and cancer in the digestive tract and lungs [1]. Chromium can exist in oxidation states ranging from –2 to +6. In aquatic environments, trivalent Cr(III) and hexavalent Cr(VI) are the major forms of chromium. Cr(VI) exists as extremely soluble and highly toxic chromate ions ($HCrO_4^-$, $Cr_2O_7^{2-}$), whereas Cr(III) is considered as relatively stable and less dangerous due to its low solubility and mobility in soils and aquifers [2].

Chromium contamination of drinking water resources is a serious environmental problem. In many countries, chromium is present in groundwater at concentrations exceeding the guidelines of the World Health Organization (0.05 mg/L), causing serious health problems [1]. Chromium is present in the effluents from electroplating, leather, mining, dyeing, fertilizer and photography industries [3]. Several methods are utilized to remove Cr(VI) from the industrial wastewater. Conventional separation techniques, such as electrochemical precipitation, slow sand filtration, ion exchange, reverse osmosis and solvent extraction, have many disadvantages including high cost, possible production of secondary toxic compounds, and generation of sludge leading to high disposal costs [4]. Adsorption separation has been widely used in environmental chemistry, owing to its relatively low cost, simplicity of design/operation and pollutant removal to low concentrations [3].

Activated carbon fiber (ACF) is a kind of activated carbons. ACF has thin-fiber shape with a diameter of 10 μm and contains inner porous network of mesopores and micropores [5]. ACF is widely applied for water purification because of fast intra-particle adsorption compared with powdered and granular forms of activated carbon [6]. ACF has been used for the removal of contaminants, such as heavy metals, organic compounds, microorganisms, and oxyanions, by many researchers [7-11]. Limited studies have been performed to use raw and/or functionalized ACF as an adsorbent for the removal of chromium from aqueous solutions [12-14]. Aggarwal et al. [15] used both raw and nitric



**Received** March 10, 2014 **Accepted** May 27, 2014

†Corresponding Author
E-mail: songbkim@snu.ac.kr
Tel: +82-2-880-4587 Fax: +82-2-873-2087

acid-treated ACF to perform adsorption isotherm studies for Cr(III) and Cr(VI) removal. Park et al. [16] examined the adsorption of Cr(VI) to surface functionalized ACF using kinetic batch experiments. Mohan et al. [17] performed the equilibrium and kinetic batch experiments to examine the Cr(III) adsorption to ACF. Further research works are needed to improve our knowledge regarding the performance of ACF in chromium removal from aqueous solutions.

The aim of this study was to investigate the adsorption of Cr(VI) from aqueous solutions to ACF using both batch and flow-through column experiments and to compare with previously reported research works. The characteristics of ACF were elucidated using field emission scanning electron microscopy (FE-SEM), nitrogen gas ($N_2$) adsorption-desorption experiment, and Fourier transform infrared (FTIR) spectrometer. Batch experiments were performed to examine the effect of reaction time, initial Cr(VI) concentration, and pH on the adsorption of Cr(VI) to ACF. Kinetic and equilibrium isotherm models were used to analyze the batch experimental data. Flow-through experiments were performed to examine the removal of Cr(VI) in the columns containing ACF. Mathematical models were used to analyze the column experimental data.

## 2. Materials and Methods

### 2.1. Characterization of Activated Carbon Fiber

The cotton-based ACF was purchased from Korea Activated Carbon Fiber Ltd. FESEM analysis was performed using a field emission scanning electron microscope (SUPRA 55VP; Carl Zeiss, Oberkochen, Germany). $N_2$ adsorption-desorption experiments were performed using a surface area analyzer (BELSORP-max; BEL Japan Inc., Osaka, Japan) after the sample was pretreated at 120°C. From the $N_2$ adsorption-desorption isotherms, the specific surface area, average pore diameter, total pore volume, and mesopore volume were determined by Brunauer-Emmett-Teller (BET) and Barrett-Joyner-Halenda analyses. Infrared spectra were recorded on a Nicolet 6700 FTIR spectrometer (Thermo Scientific, Waltham, MA, USA) using KBr pellets.

### 2.2. Batch Experiments

The desired Cr(VI) solution was prepared by diluting the stocking Cr(VI) solution (1,000 mg/L), which was made from potassium dichromate ($K_2Cr_2O_7$). All batch experiments were performed in 50 mL polypropylene conical tubes without pH adjustment except the experiments of pH effect. Note that pH of 100 mg/L Cr(VI) solution was around 4.9. The first batch experiments were performed at different reaction times (adsorbent dose, 0.3 g in 30 mL; initial Cr(VI) concentration ($C_0$), 100 mg/L). The tubes were shaken at 25°C and 100 rpm using a shaking incubator (Daihan Science, Wonju, Korea). In the experiments, samples were collected at 1, 2, 4, 6, 8, 12, and 24 hr after reaction. The samples were filtered through a 0.45-μm membrane filter, and Cr(VI) concentration was measured by UV/Vis spectrophotometer (Helios, Thermo Scientific) using diphenylcarbazide method. The second batch experiments were conducted at different concentrations of Cr(VI) solution. The adsorbent (0.3 g) was added to 30 mL of Cr(VI) solution (initial Cr(VI) concentration, 5–500 mg/L). The samples were collected 24 hr after reaction. The third batch experiments (adsorbent dose, 0.3 g in 30 mL; initial Cr(VI) concentration, 100 mg/L) were conducted at various solution pH ranging from 2.6 to 9.9. The samples were collected 24 hr after reaction. In the pH experiments, 0.1 M NaOH and 0.1 M HCl solutions were used for adjusting the pH from 2.6 to 9.9. The pH was measured with a pH probe (9107BN, Thermo Scientific). All experiments were performed in triplicate.

### 2.3. Column Experiments

Flow-through column experiments were performed at two different flow conditions (flow rate, 0.5 and 1.0 mL/min) using a polyethylene column (column length, 10 cm; inner diameter, 1.5 cm) packed with ACF. Prior to the experiments, the packed column was flushed upward using a HPLC pump (Series II pump; Scientific Systems Inc., State College, PA, USA) with 10 bed volumes of deionized water until steady state flow conditions were established. Then, Cr(VI) solution was introduced downward continuously to the packed column. Portions of the effluent were collected using the auto collector (Retriever 500; Teledyne Isco Inc., Lincoln, NE, USA) at a regular interval up to 760 and 2,700 min in the column experiments 1 and 2, respectively. The concentration of Cr(VI) was measured by UV/Vis spectrophotometer (Helios, Thermo Scientific) using diphenylcarbazide method.

### 2.4. Data Analysis

All of the parameters of the models were estimated using MS Excel 2010 with the solver add-in function incorporated into the program. The model parameter values were determined by nonlinear regression. The determination coefficient ($R^2$), chi-square coefficient ($\chi^2$), and sum of squared errors (SSE) were used to analyze the data and confirm the fit to the model. The expressions of $R^2$, $\chi^2$, and SSE are given below:

$$R^2 = \frac{\sum_{i=1}^{m}(y_c - \overline{y}_e)_i^2}{\sum_{i=1}^{m}(y_c - \overline{y}_e)_i^2 + \sum_{i=1}^{m}(y_c - y_e)_i^2} \quad (1)$$

$$\chi^2 = \sum_{i=1}^{m}\left[\frac{(y_e - y_c)^2}{y_c}\right]_i \quad (2)$$

$$SSE = \sum_{i=1}^{m}(y_e - y_c)_i^2 \quad (3)$$

where $y_c$ is the calculated adsorption capacity from the model, $y_e$ is the measured adsorption capacity from the experiment, and $\overline{y}_e$ is the average of the measured adsorption capacity.

## 3. Results and Discussion

### 3.1. Characteristics of ACF

The FESEM image of ACF showed that ACF had a thin-fiber shape with a diameter of 10 μm (Fig. 1(a)). From $N_2$ adsorption-desorption isotherm (Fig. 1(b)), the BET surface area of ACF was determined to be 1,123.0 $m^2/g$ with total pore volume of 0.52 $cm^3/g$, mesopore volume of 0.09 $cm^3/g$, and average pore diameter of 1.85 nm. In the FTIR spectra (Fig. 1(c)), two peaks at 2,950 and 2,880 (/cm) corresponded to symmetric stretching vibrations of $–CH_2$ and stretching vibrations of –CH, respective-

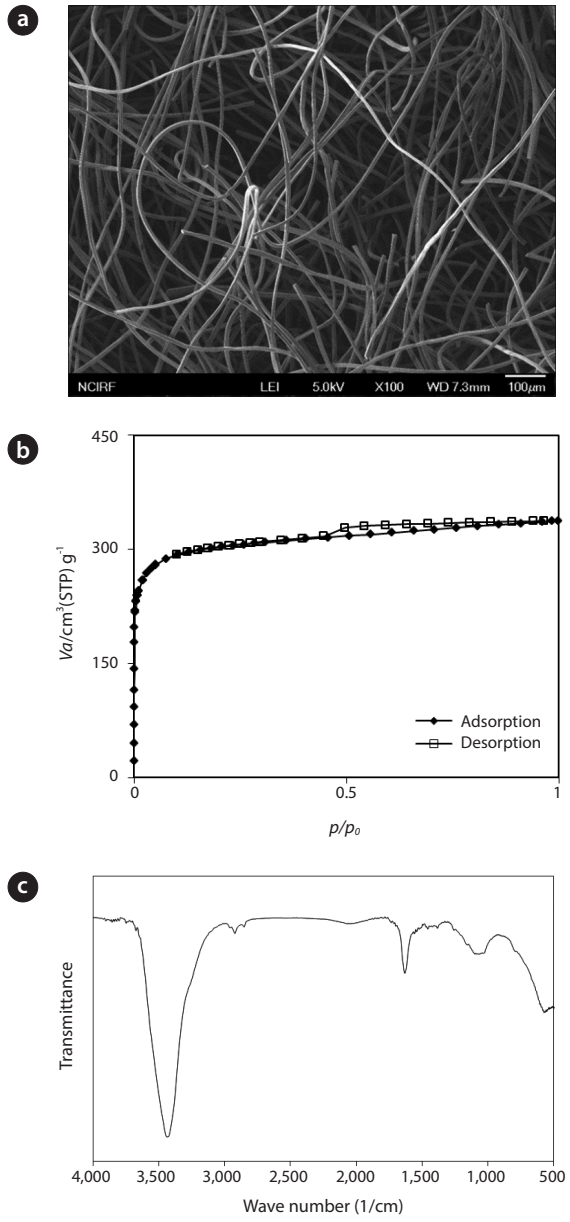


**Fig. 1.** Activated carbon fiber used in the experiments: (a) field emission scanning electron microscope image (bar = 100 μm); (b) $N_2$ adsorption-desorption isotherm; (c) Fourier transformed infrared spectra.

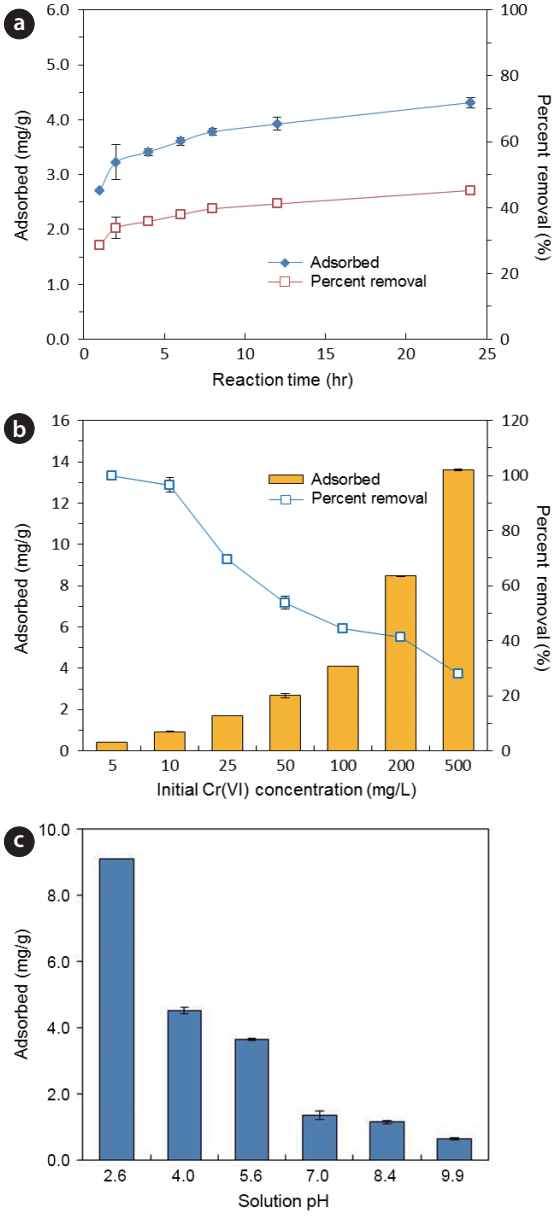


**Fig. 2.** Cr(VI) removal by activated carbon fiber: (a) effect of reaction time, (b) effect of initial Cr(VI) concentration, and (c) effect of solution pH.

ly. In addition, the band of C = O were observed at 1,680-1,720 (/cm) [10].

### 3.2. Effects of Reaction Time, Cr(VI) Concentration, and Solution pH

The effect of reaction time on the adsorption of Cr(VI) to ACF is shown in Fig. 2(a). At 1 hr of reaction time, the adsorption capacity was 2.71 mg/g with the percent removal of 28.5%. The adsorption capacity increased to 3.60 mg/g with the percent removal of 37.8% at 6 hr. At 12 hr, the adsorption capacity and percent removal were 3.92 mg/g and 41.1%, respectively. At 24 hr, the adsorption capacity was 4.31 mg/g with the percent removal of 45.2%. Similar results were reported by Park and Kim [13], who showed that adsorption percent of Cr(VI) to ACF increased from 3% to 27% with increasing reaction time from 10 to 180 min. Park and Jung [18] also reported that the percent removal of Cr(VI) in ACF increased from 49% to 87% as the reaction time increased from 10 to 180 min.

The effect of the initial concentrations of Cr(VI) on the Cr(VI) sorption to ACF is presented in Fig. 2(b). The Cr(VI) removal was highly concentration dependent. As the Cr(VI) concentration increased, the adsorption capacity increased rapidly. At the lowest concentration of 5 mg/L, the adsorption capacity was 0.42 mg/g.

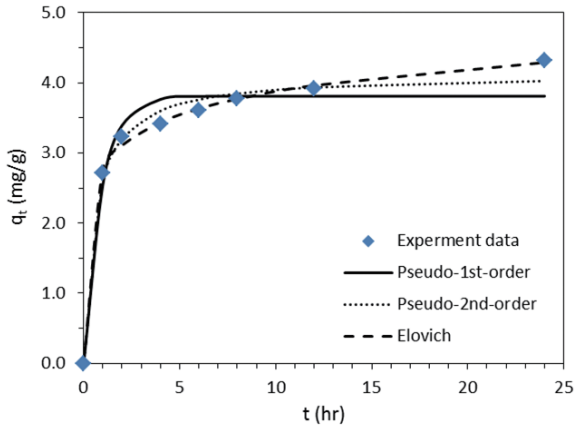


**Fig. 3.** Kinetic model analysis. Model parameters are provided in Table 1.

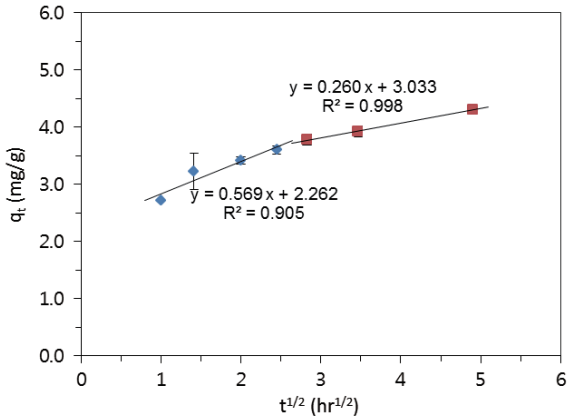


**Fig. 4.** Intra-particle diffusion model analysis. Model parameters are provided in Table 2.

As the Cr(VI) concentration increased to 100 mg/L, the adsorption capacity increased to 4.09 mg/g. At the highest concentration of 500 mg/L, the adsorption capacity increased to 13.60 mg/g. Meanwhile, the percent removal decreased with increasing Cr(VI) concentration. The percent removal was 100% at 5 mg/L and decreased to 28.1% at 500 mg/L. Similar findings were reported by Aggarwal et al. [15] who showed that the amount of Cr(VI) adsorbed onto ACF increased gradually from 5 to 20 mg/g with increasing Cr(VI) concentration from 20 to 1,000 mg/L.

The effect of solution pH on the adsorption of Cr(VI) to ACF is given in Fig. 2(c). The adsorption capacity at pH 2.6 was 9.09 mg/g. At pH 4.0, the adsorption capacity was 4.43 mg/g. As the solution pH increased to 7.0, the adsorption capacity approached 1.20 mg/g. As the solution pH further increased to 9.9, the adsorption capacity reached 0.66 mg/g. In aqueous solution, Cr(VI) is present in the anionic forms, $HCrO_4^-$ and $CrO_4^{2-}$, depending on the pH. $HCrO_4^-$ is dominant species of Cr(VI) at pH < 6, which gradually transformed into $CrO_4^{2-}$ as the pH increases [1]. The sorption of Cr(VI) to ACF was sensitive to solution pH with the highest adsorption capacity at the highly acidic solution pHs. This result could be attributed to the protonation of ACF surfaces at acidic pHs, resulting in the electrostatic attraction between positively-charged ACF surfaces and negatively-charged chromium ions ($HCrO_4^-$). As the pH increased, the surfaces of ACF became negatively-charged, and so the electrostatic repulsion between ACF surfaces and chromium ions ($CrO_4^{2-}$) became strong, resulting in the decrease of Cr(VI) sorption [19]. Note that the point of zero charge ($pH_{pzc}$) of ACF was reported to be 4.3 [20]. Our result agreed well with the report of Ko and Choi [14] who showed that Cr(VI) adsorption to ACF decreased from 1.3 mmol/g to near zero with increasing pH from 1.5 to 12.7. Other researchers also reported that the adsorption of Cr(VI) to ACF was maximal at pH 3 and decreased with increasing pH [12].

### 3.3. Kinetic, Intra-particle Diffusion, and Equilibrium Isotherm Model Analyses

The reaction time data were analyzed using the following nonlinear forms of pseudo-first-order (Eq. (4)), pseudo-second-order (Eq. (5)), and Elovich (Eq. (6)) kinetic models:

$$q_t = q_e\left(1-e^{-k_1 t}\right) \tag{4}$$

$$q_t = \frac{k_2 q_e^{\,2} t}{1+k_2 q_e t} \tag{5}$$

$$q_t = \frac{1}{\beta}\ln(\alpha\beta)+\frac{1}{\beta}\ln t \tag{6}$$

where $q_t$ is the amount of Cr(VI) removed at time t, $q_e$ is the amount of Cr(VI) removed per unit mass of adsorbent at equilibrium, $k_1$ is the pseudo-first-order rate constant, $k_2$ is the pseudo-second-order velocity constant, $\alpha$ is the initial adsorption rate constant, and $\beta$ is the Elovich adsorption constant.

The kinetic data and model fits for Cr(VI) sorption to ACF are shown in Fig. 3. Model parameters for the pseudo-first-order, pseudo-second-order, and Elovich models are provided in Table 1. In the pseudo-first-order model, the value of $q_e$ was 3.81 mg/g, and the value of $k_1$ was 1.11 (/hr). The value of $q_e$ from the pseudo-second-order model was larger than that from the pseudo-first-order model. The value of $q_e$ was 4.12 mg/g, and the value of $k_2$ was 0.42 g/mg/hr, respectively. In the Elovich model, the values of $\alpha$ and $\beta$ were 162.65 mg/g/hr and 2.10 g/mg, respectively. The values of $R^2$, $\chi^2$, and SSE indicate that the Elovich model was the most suitable for describing the data.

**Table 1.** Kinetic model parameters obtained from model fitting to experimental data

| Pseudo-first-order | | | | | Pseudo-second-order | | | | | Elovich | | | | |
|---|---|---|---|---|---|---|---|---|---|---|---|---|---|---|
| $q_e$ (mg/g) | $k_1$ (/hr) | $R^2$ | SSE | $\chi^2$ | $q_e$ (mg/g) | $k_2$ (g/mg/hr) | $R^2$ | SSE | $\chi^2$ | $\alpha$ (mg/g/hr) | $\beta$ (g/mg) | $R^2$ | SSE | $\chi^2$ |
| 3.81 | 1.11 | 0.695 | 0.487 | 0.129 | 4.12 | 0.42 | 0.903 | 0.159 | 0.042 | 162.65 | 2.10 | 0.987 | 0.022 | 0.007 |

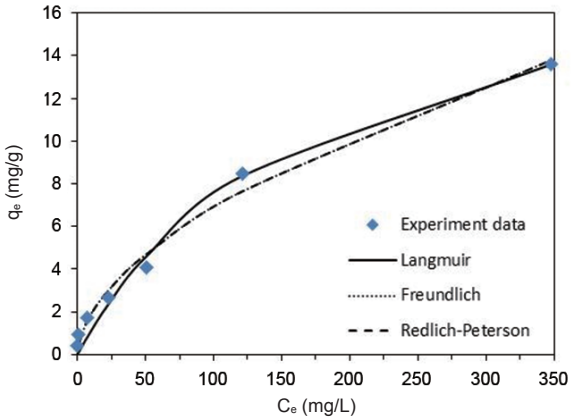


**Fig. 5.** Equilibrium isotherm model analysis. Model parameters are provided in Table 3.

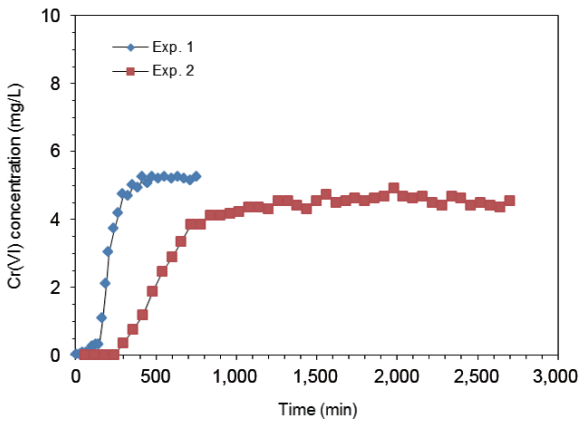


**Fig. 6.** Breakthrough curves of Cr(VI) obtained from flow-through column experiments. Experimental conditions and results are provided in Table 4.

The reaction time data were also analyzed by the following intra-particle diffusion model:

$$q_t = K_i t^{1/2} + I \tag{7}$$

where $K_i$ is the intra-particle diffusion rate constant, and $I$ is the intercept related to the thickness of the boundary layer. The kinetic sorption data analyzed by the intra-particle diffusion model is shown in Fig. 4, indicating that the plots were composed of two line segments. The first line in the plot indicates boundary layer adsorption, while the second line describes the intra-particle diffusion [21]. Model parameters for the intra-particle diffusion model are presented in Table 2. The diffusion model was well fitted to the data, with coefficients of determination ($R^2$) of 0.905 (first line) and 0.998 (second line). Values of $K_i$ for the first and second lines were 0.57 and 0.26 mg/g/hr$^{1/2}$, respectively. The first line in the plot indicates boundary layer adsorption, while the second line describes the intra-particle diffusion [21].

The Cr(V) concentration data were analyzed using the following nonlinear forms of Freundlich (Eq. (8)), Langmuir (Eq. (9)), and Redlich–Peterson (Eq. (10)) isotherm models:

$$q_e = K_F C_e^{1/n} \tag{8}$$

$$q_e = \frac{Q_m K_L C_e}{1 + K_L C_e} \tag{9}$$

$$q_e = \frac{K_R C_e}{1 + a_R C_e^{g}} \tag{10}$$

where $C_e$ is the concentration of Cr(VI) in the aqueous solution at equilibrium, $K_F$ is the distribution coefficient, $1/n$ is the Freundlich constant, $Q_m$ is the maximum mass of Cr(VI) removed per unit mass of adsorbent (removal capacity), $K_L$ is the Langmuir constant related to the binding energy, $K_R$ is the Redlich–Peterson constant related to the adsorption capacity, $a_R$ is the Redlich–Peterson constant related to the affinity of the binding sites, and $g$ is the Redlich–Peterson constant related to the adsorption intensity.

**Table 2.** Intra-particle diffusion model parameters obtained from model fitting to experimental data

| Boundary layer adsorption | | | Intra-particle diffusion | | |
|---|---|---|---|---|---|
| $K_{i,1}$ (mg/g/hr$^{0.5}$) | $I$ | $R^2$ | $K_{i,2}$ (mg/g/hr$^{0.5}$) | $I$ | $R^2$ |
| 0.57 | 2.26 | 0.905 | 0.26 | 3.03 | 0.998 |

The equilibrium data and isotherm model fits for Cr(VI) sorption to ACF are shown in Fig. 5. The equilibrium isotherm parameters for the Langmuir, Freundlich, and Redlich–Peterson models are summarized in Table 3. The values of $R^2$, $\chi^2$, and SSE indicate that both Freundlich and Redlich–Peterson models were suitable for describing the data. Note that the Redlich–Peterson model fit was superimposed on the Freundlich fit (Fig. 5). The Redlich–Peterson model can be reduced to the Freundlich model if $K_R$ and $a_R$ are much greater than unity [22]. In the Freundlich model, the value of $K_F$ was 0.52 L/g, which corresponded well to the value of $K_R/a_R$ in the Redlich–Peterson model. The value of $1/n$ was equivalent to the value (0.56) of (1–$g$). The adsorption capacity ($q_m$) was calculated from $K_F$ and $1/n$ using the following equation [23]:

$$q_m = K_F C_0^{1/n} \tag{11}$$

The value of $q_m$ was calculated to be 6.85 mg/g. From the Langmuir model, the maximum adsorption capacity ($q_m$) was determined to be 20.54 mg/g, which was in the ranges of the Cr(VI) adsorption capacity of raw ACF and surface-modified ACF (0.138–45 mg/g) reported in the literature [7, 12, 13, 15, 16, 18].

### 3.4. Cr(VI) Removal in Flow-Through Conditions

The BTCs of Cr(VI) obtained from the flow-through column experiments are shown in Fig. 6. The experimental conditions and results are presented in Table 4. In the column experiments, the empty bed contact time (EBCT, min) was determined as following:

$$EBCT = \frac{V_r}{Q} \tag{12}$$

where $V_r$ is the fixed-bed volume, and $Q$ is the volumetric flow rate. The total mass of Cr(VI) injected into column ($M_{total}$) during

**Table 3.** Equilibrium isotherm model parameters obtained from model fitting to experimental data

| Langmuir | | | | | Freundlich | | | | | Redlich-Peterson | | | | | | |
|---|---|---|---|---|---|---|---|---|---|---|---|---|---|---|---|---|
| $q_m$ (mg/g) | $K_L$ (L/mg) | $R^2$ | SSE | $\chi^2$ | $K_F$ (L/g) | 1/n | $R^2$ | SSE | $\chi^2$ | $K_R$ (L/g) | $a_R$ (L/mg) | $K_R/a_R$ (mg/g) | g | $R^2$ | SSE | $\chi^2$ |
| 20.54 | 0.0057 | 0.985 | 2.123 | 1.824 | 0.52 | 0.56 | 0.987 | 1.840 | 1.104 | 1,255.89 | 2,401.28 | 0.52 | 0.44 | 0.987 | 1.840 | 1.104 |

**Table 4.** Flow-through column experimental conditions and results for Cr(VI) removal by activated carbon fiber

| Exp. | $V_r$ ($cm^3$) | Q (mL/min) | EBCT (min) | $t_{total}$ (min) | $C_0$ (mg/L) | $M_{total}$ (mg) | $C_{cap}$ (mg) | $M_f$ (g) | $q_a$ (mg/g) |
|---|---|---|---|---|---|---|---|---|---|
| 1 | 17.7 | 1.0 | 17.7 | 760 | 10 | 7.6 | 4.68 | 1.99 | 2.35 |
| 2 | 17.7 | 0.5 | 35.4 | 2,700 | 10 | 13.5 | 8.35 | 1.99 | 4.20 |

the experiment was calculated as following:

$$M_{total} = \frac{C_0 Q t_{total}}{1000} \quad (13)$$

where $C_0$ is the influent concentration of Cr(VI), and $t_{total}$ is the total flow time. The column capacity for Cr(VI) removal at a given flow rate and influent concentration of Cr(VI) ($C_{cap}$) was quantified as following:

$$C_{cap} = \frac{Q}{1000}\int_{t=0}^{t=t_{total}} (C_0 - C)\,dt \quad (14)$$

where $C$ is the effluent concentration of Cr(VI). The mass of Cr(VI) removed per unit mass of filter materials in the column ($q_a$) was determined as following:

$$q_a = \frac{C_{cap}}{M_f} \quad (15)$$

where $M_f$ is the mass of filter materials in the column.

In the case of Exp. 1, no breakthrough of Cr(VI) was observed from the experiment until 30 min. The effluent concentration of Cr(VI) rose slowly up to 150 min and then increased drastically with time, reaching the half (5.0 mg/L) of the influent concentration at 360 min. Thereafter, the effluent concentration of Cr(VI) remained relatively constant at 5.1–5.2 mg/L until 760 min. In Exp. 1, the Cr(VI) adsorption capacity of ACF in the column was determined to be 2.35 mg/g. In the case of Exp. 2, no breakthrough of Cr(VI) was observed until 240 min. The effluent concentration of Cr(VI) increased gradually up to 1,020 min and then fluctuated between 4.5–4.9 mg/L up to 2,700 min. In Exp. 2, the Cr(VI) adsorption capacity of ACF in the column was calculated to be 4.20 mg/g, which was 1.8 times greater than that of Exp. 1. Note that the EBCT of Exp. 2 (35.4 min) was larger than that (17.7 min) of Exp.1 (Table 4). The Cr(VI) adsorption capacities from the flow-through column experiments were one order of magnitude lower than that (20.54 mg/g) from the batch experiments. This result could be attributed to the fact that the contact time between an adsorbent (ACF) and a contaminant (Cr(VI)) in the flow-through column experiment was far shorter than that in the batch experiment.

## 4. Conclusions

In this study, the sorption of Cr(VI) to ACF was examined using batch and column experiments. The batch experiments showed that the maximum adsorption capacity of Cr(VI) to ACF was 20.54 mg/g. The adsorption of Cr(VI) to ACF was sensitive the sorption of Cr(VI) to ACF was sensitive to solution pH with the highest adsorption capacity at the highly acidic solution pHs. Kinetic model analysis showed that the Elovich model was the most suitable for describing the kinetic data. Equilibrium isotherm model analysis demonstrated that both Freundlich and Redlich–Peterson models were suitable for describing the equilibrium data. The column experiments showed that the adsorption capacities of ACF were in the range of 2.35–4.20 mg/g in the given experimental conditions. This study demonstrated that ACF was effective for the removal of Cr(VI) in the batch and flow-through column conditions.

## Acknowledgments

This work was supported by the National Research Foundation of Korea funded by the Ministry of Education, Republic of Korea (No. 2013-008829).

## References

1. Richard FC, Bourg A. Aqueous geochemistry of chromium: a review. *Water Res.* 1991;25:807-816.
2. Zhitkovich A. Chromium in drinking water: sources, metabolism, and cancer risks. *Chem. Res. Toxicol.* 2011;24:1617-1629.
3. Sharma SK, Petrusevski B, Amy G. Chromium removal from water: a review. *J. Water Supply: Res. Technol. AQUA* 2008;57:541-553.
4. Albadarin AB, Mangwandi C, Al-Muhtaseb AA, Walker GM, Allen SJ, Ahmad MN. Kinetic and thermodynamics of chromium ions adsorption onto low-cost dolomite adsorbent. *Chem. Eng. J.* 2012;179:193-202.
5. Suzuki M. Activated carbon fiber: fundamentals and applications. *Carbon* 1994;32:577-586.
6. Osmond NM. Activated carbon fibre adsorbent materials. *Adsorpt. Sci. Technol.* 2000;18:529-539.
7. Ko YG, Choi US, Kim JS, Park YS. Novel synthesis and characterization of activated carbon fiber and dye adsorption modeling. *Carbon* 2002;40:2661-2672.
8. Park SJ, Jang YS. Preparation and characterization of activated carbon fibers supported with silver metal for antibacterial

behavior. *J. Colloid Interface Sci*. 2003;261:238-243.
9. Harry ID, Saha B, Cumming IW. Effect of electrochemical oxidation of activated carbon fiber on competitive and non-competitive sorption of trace toxic metal ions from aqueous solution. *J. Colloid Interface Sci*. 2006;304:9-20.
10. Li K, Li Y, Zheng Z. Kinetics and mechanism studies of p-nitroaniline adsorption on activated carbon fibers prepared from cotton stalk by $NH_4H_2PO_4$ activation and subsequent gasification with steam. *J. Hazard. Mater*. 2010;178:553-559.
11. Zhang L, Wan L, Chang N, et al. Removal of phosphate from water by activated carbon fiber loaded with lanthanum oxide. *J. Hazard. Mater*. 2011;190:848-855.
12. Ko KR, Ryu SK, Park SJ. Effect of ozone treatment on Cr(VI) and Cu(II) adsorption behaviors of activated carbon fibers. *Carbon* 2004;42:1864-1867.
13. Park SJ, Kim YM. Influence of anodic treatment on heavy metal ion removal by activated carbon fibers. *J. Colloid Interface Sci*. 2004;278:276-281.
14. Ko YG, Choi US. Observation of metal ions adsorption on novel polymeric chelating fiber and activated carbon fiber. *Sep. Purif. Technol*. 2007;57:338-347.
15. Aggarwal D, Goyal M, Bansal RC. Adsorption of chromium by activated carbon from aqueous solution. *Carbon* 1999;37:1989-1997.
16. Park SJ, Park BJ, Ryu SK. Electrochemical treatment on activated carbon fibers for increasing the amount and rate of Cr(VI) adsorption. *Carbon* 1999;37:1223-1226.
17. Mohan D, Singh KP, Singh VK. Trivalent chromium removal from wastewater using low cost activated carbon derived from agricultural waste material and activated carbon fabric cloth. *J. Hazard. Mater*. 2006;135:280-295.
18. Park SJ, Jung WY. Removal of chromium by activated carbon fibers plated with copper metal. *Carbon Sci*. 2001;2:15-21.
19. Huang L, Zhou S, Jin F, Huang J, Bao N. Characterization and mechanism analysis of activated carbon fiber felt-stabilized nanoscale zero-valent iron for the removal of Cr(VI) from aqueous solution. *Colloids Surf. A Physicochem. Eng. Asp*. 2014;447:59-66.
20. Cardenas-Lopez C, Camargo G, Giraldo L, Moreno-Pirajan JC. Design of an adsorbent employing activated carbon fiber to remove lead. *Eclét. Quím*. 2007;32:61-71.
21. Bajpai SK, Armo MK. Equilibrium sorption of hexavalent chromium from aqueous solution using iron(III)-loaded chitosan-magnetite nanocomposites as novel sorbent. *J. Macromol. Sci. A Pure Appl. Chem*. 2009;46:510-520.
22. Zhang L, Hong S, He J, Gan F, Ho YS. Adsorption characteristic studies of phosphorus onto laterite. *Desalination Water Treat*. 2011;25:98-105.
23. Halsey G. Physical adsorption on non-uniform surfaces. *J Chem. Phys*. 2004;16:931-937.